International Journal Of
Industrial Electronics Control and Optimization
Print ISSN: 3517-2645
Online ISSN: 3568-2645
Homepage: https://ieco.usb.ac.ir/

Design a High-Efficiency Rectifier Circuit Using Various Couplers for Microwave Power Transmission

Mohammad M. Fakharian

Faculty of Engineering, University of Garmsar, Garmsar, Iran
Corresponding author's email: fakharian@fmgarmsar.ac.ir

Article Info

Article type:
Research Article

Article history:
Received: 08-February-2025
Received in revised form: 09-April-2025
Accepted: 05-June-2025
Published online: 21-March-2026

Keywords:
Rectifier circuit,
RF-DC efficiency,
Microwave coupler,
Wide range of input power.

ABSTRACT

This paper presents an optimized microwave rectifier circuit that integrates various couplers to enhance RF-to-DC conversion efficiency. A comprehensive theoretical analysis and performance evaluation of different microwave couplers are conducted to determine their impact on power distribution and impedance matching. The study demonstrates that incorporating couplers into the rectifier circuit effectively reduces reflected power over a broad input power range. Among the evaluated configurations, the rectifier incorporating a branch-line coupler (BLC) exhibits superior RF-to-DC efficiency over a wide range of operating frequencies, input power levels, and output loads, ensuring broad impedance matching. To validate the proposed design, a rectifier circuit based on the BLC is implemented and fabricated at 2.45 GHz. The prototype consists of two identical sub-rectifying networks connected to the two output ports of the coupler, with the isolated port grounded. Experimental results indicate that the rectifier consistently achieves efficiency levels exceeding 50% for input power levels ranging from 0 to 12.5 dBm. Additionally, the design maintains high efficiency across a frequency range of 2.16 to 2.96 GHz. These findings underscore the potential of BLC-based rectifiers for high-efficiency microwave power transmission systems, offering enhanced energy harvesting capabilities and improved system performance.

I. Introduction

Recently, microwave power transmission (MPT) has been a topic of research interest for a variety of applications in near-field and far-field categories, such as radio frequency (RF) identification, energy harvesting, and wireless sensor networks [1-5]. In MPT systems, rectennas play a significant role, and their efficiencies primarily depend on rectifier circuits. Therefore, the design of high-efficiency rectifying circuits is crucial for MPT systems. As a key component of MPT systems, rectifiers are used to convert RF power into direct current (DC) power. The rectifying circuit performance is typically verified by its RF-DC conversion efficiency.

So far, to enhance and optimize the efficiency of the rectifiers, many studies in analytical models and different types of structures have been presented [7-12]. To improve efficiency, Class-F rectifiers [7] were introduced by suppressing the power of harmonic components. In [8], a technique of harmonic recycling was employed, while in [9], a terminated diode with harmonic behavior was applied for this purpose. In [10], a high-efficiency rectifier with a load of Class-F, using a charge pump circuit, was designed. In [11], a computationally efficient iterative method with fast convergence for rectifier modification was introduced. A C-band rectifier utilizing a single silicon-based Schottky diode is proposed in [12]. In [13], a high-input power (>30 dBm) rectifier circuit for 2.45 GHz was presented, using a rectifier circuit based on a GaAs FET and a Schottky diode together as the rectification components. These designed rectifiers are typically improved for single working frequency, fixed output load, and narrow input power level, especially when the rectifier is integrated with a narrow-band antenna. On the other hand, the available RF energy is usually not continuous, causing variations in operating conditions that lead to input impedance changes and reduced efficiency due to the nonlinear characteristics of rectification. To enhance rectifier performance under various operating conditions, several structures and techniques have been developed to broaden bandwidth [14-19], extend the load range [20], improve the operating power range [21-26], or achieve a

combination of these improvements [27-30]. In [31-34], rectifiers were designed by incorporating multiple sub-rectifiers optimized in parallel to accommodate a wide range of input power. As well as, GaAs pHEMT [35] and Varactor diodes [23] have been employed to enhance and extend the maximum breakdown power and the matching performance. Moreover, based on previous works [26, 27], and [28], a rectifier circuit integrated with a suitable coupler can simultaneously operate under varying input power and output load conditions by recycling the reflected power from a sub-rectifier that is not perfectly matched. For example, in [27], the rectifier contains two sub-rectifier networks and a branch-line coupler (BLCoupler) with a grounded isolation port to enhance efficiency. Nevertheless, other couplers such as tee power divider (TCoupler), Wilkinson divider (WDCoupler), rat-race coupler (RRCoupler), coupled-line coupler (CLCoupler), and lange coupler (LCoupler), can also be used for rectifiers, and then the efficiency comparisons between them with the different couplers can also be verified and studied. Recently, a dual-channel RF-DC rectifier circuit is presented at 2.45 Ghz with a 2:1 power distribution ratio in a Wilkinson power splitter in [36], however, in this work as well, no comparison has been made with other coupler structures.

In this paper, various couplers are analyzed and compared for developing and designing a high-efficiency rectifying circuit. In these designs, the two output ports of the coupler are connected to two identical sub-rectifying networks, while the isolated port is grounded. This rectifier configuration maintains high RF-DC efficiency over a broad range of operating frequencies, input power levels, and output loads, resulting in improved impedance matching [37]. Section II presents the topology and theoretical analysis of couplers. Section III discusses rectifier designs and evaluates their RF-DC efficiency with and without different couplers. For validation, Section IV describes the implementation and fabrication of a prototype rectifier circuit based on a BLCoupler at 2.45 GHz. Finally, the conclusions are summarized in Section V.

II. Topology and Theoretical Analysis of Couplers

According to [27], the topology of the rectifier circuit based on two branches with a coupler is shown in Fig. 1. For each branch, it comprises a matching network (MN), a sub-rectifier, and a DC-pass block to weaken the rectified voltage harmonics and output a smooth voltage on the resistances R_{L1-2}. Two identical sub-rectifiers using Schottky diodes HSMS2850 from Avago [38] are linked to the output ports of the MN. This diode is a good choice for designing a rectifier circuit, due to its electrical characteristics, such as low forward voltage, fast switching, low reverse leakage current, high-frequency suitability, and compact size. The input impedances Zin1 and Zin2 of the sub-rectifiers vary when the input operating frequency, input power, and output load change, resulting in an impedance mismatch. The designed topology can enhance matching performance, increase RF-DC efficiency, and reduce the power loss caused by impedance mismatch.

To study the operating principle of the designed rectifier with the different couplers or power dividers, it should first discuss the properties of the common types of couplers and power dividers.

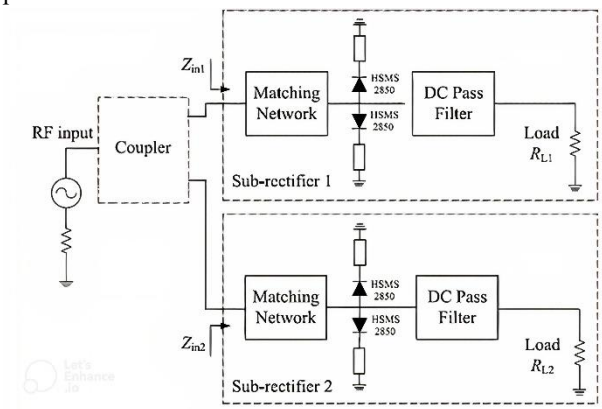

Fig. 1. Block diagram of the rectifier with coupler.

A. TCoupler and WDCoupler

The T-junction power divider (TCoupler) and Wilkinson power divider (WDCoupler) are three-port networks that can be used for power combining or division, as well as automatic impedance transformation in the rectifying circuit [28]. In this regard, a symmetric 3-dB lossless TCoupler and a symmetric two-way WDCoupler with an isolation resistor of 2Rs are used, as shown in Fig. 2(a) and 2(b), respectively. In the WDCoupler, if a mismatch occurs, the reflected power is dissipated through the isolation resistor. Compared with [28], the two symmetric branches each have an electrical length of 90°, a1 is the input wave to the couplers, ZL1 and ZL2 represent the input impedances of the two sub-rectifying networks, and Rs is set to 50 Ω. According to [28] and [39], output waves d1 and d2 can be described as follows:

$$d_1 = d_2 = -j\frac{a_1}{\sqrt{2}}. \quad (1)$$

Since the output load ZL1-2 changes and mismatching are produced, the reflected waves ar1 and ar2 are

$$a_{r1} = a_{r2} = -j\frac{a_1}{\sqrt{2}}\Gamma \quad (2)$$

The waves ar1 and ar2 are transmitted to the TCoupler or WDCoupler and then delivered to port 1; consequently, the power loss of the couplers can be determined as

$$P_{lossT} = \frac{1}{2}|a_{r1}|^2 + \frac{1}{2}|a_{r2}|^2 = \frac{1}{2}|\Gamma|^2|a_1|^2, \quad (3)$$

$$P_{lossWD} = \frac{1}{2}|a_{r1}|^2 + \frac{1}{2}|a_{r2}|^2 + P_{2Rs} = \frac{1}{2}|\Gamma|^2|a_1|^2 + P_{2Rs}. \quad (4)$$

In equation (4), Since the output load ZL1-2 is variable, the isolation resistor is not equivalent to being open in an ideal case, and it is considered in the losses. In the following,

as illustrated in Fig. 2, in the rectifier with the TCoupler, the reflected power is $P_{lossT} = P_{ref} = |\Gamma|^2 P_{inc}$, while with the WDCoupler is $P_{lossWD} = P_{ref} = |\Gamma|^2 P_{inc} + P_{2Rs}$, the power injected to the subrectifiers Pin is equal to $(1 - |\Gamma|^2) \times P_{inc}$ for TCoupler and $(1 - |\Gamma|^2) \times P_{inc} - P_{2Rs}$ for WDCoupler, while the incident power is equal to $\frac{|a_1|^2}{2}$.

The DC output power of the rectifier circuit with the couplers is (Pin ×ηPin), where ηPin presents the RF-DC efficiency of the sub-rectifying networks at the inserted power Pin. Thus, the efficiency ηPinc at the incident power of Pinc can be obtained by

$$\text{for TCoupler: } \eta_{P_{inc}} = \frac{P_{in} \times \eta_{P_{in}}}{P_{inc}} = (1 - |\Gamma|^2) \times \eta_{P_{in}} \quad (5)$$

$$\text{for WDCoupler: } \eta_{P_{inc}} = \frac{P_{in} \times \eta_{P_{in}}}{P_{inc}} = (1 - |\Gamma|^2) \times \eta_{P_{in}} - P_{2Rs} \times \eta_{P_{in}} \quad (6)$$

Thus, after the sub-rectifiers are specified, the RF-DC efficiency ηPinc depends on reflection coefficients Γ of the sub-rectifiers and the efficiency ηPin. Moreover, it is proved that the efficiency of the TCoupler is higher than the WDCoupler for variable loads; this is a common problem in sensor applications.

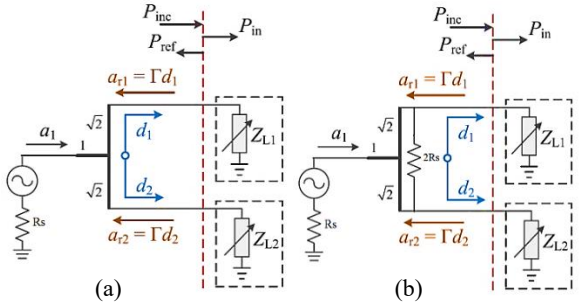

Fig. 2. The rectifier based on the symmetric a) TCoupler and b) WDCoupler.

B. RRCoupler

In this section, the rat-race coupler (RRCoupler), which is well known as a network with four ports and a phase shift of 180° between the two output ports, is verified. It can also be worked as in the in-phase outputs. The rectifiers based on the RRCoupler with the grounded isolation port are shown in Fig. 3(a) and Fig. 3(b) as an in-phase and a 180-degree hybrid. According to [39], for the ideal 3-dB 180° hybrids, the scattering matrix has the following definition:

$$[S] = \frac{-j}{\sqrt{2}} \begin{bmatrix} 0 & 1 & 1 & 0 \\ 1 & 0 & 0 & -1 \\ 1 & 0 & 0 & 1 \\ 0 & -1 & 1 & 0 \end{bmatrix}. \quad (7)$$

First, consider a wave incident with unit amplitude (a1) at port 1 (the sum port) of the RRCoupler. At the ring junction, the a1 will be distributed into two ports, which arrive at ports 2 and 3 in-phase, and Port 4 is isolated from port 1. Similar to previous couplers, we can prove the following equation:

$$\text{for in-phase: } P_{lossRR} = \frac{1}{2}|\Gamma|^2 |a_1|^2. \quad (8)$$

Now, if the signal is driven into port 2, the incident power is distributed between ports 1 and 4, although port 3 is isolated. The signals at ports 1 and 4 have 180° phase shift, and therefore, this coupler is stated as a 180-degree hybrid, and we have the following equation:

$$\text{for 180-degree hybrid: } P_{lossRR} = \frac{1}{2}|\Gamma|^2 |a_2|^2, \quad (9)$$

that in equations 1 and 2, $|a_1| = |a_2|$. Similar to the previous section, it can be concluded that the efficiency ηPinc in the incident power of Pinc is as follows: for RRCoupler:

$$\eta_{P_{inc}} = \frac{P_{in} \times \eta_{P_{in}}}{P_{inc}} = (1 - |\Gamma|^2) \times \eta_{P_{in}} \quad (10)$$

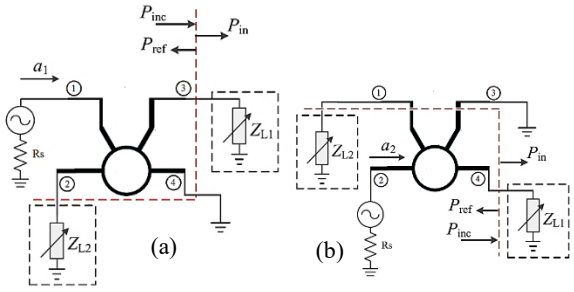

Fig. 3. The rectifier based on the RRCoupler as a) an in-phase and b) a 180-degree hybrid with grounded isolation port.

C. BLCoupler

Branch-line coupler (BLCoupler) is a 3-dB directional coupler that produces a 90° phase difference between the outputs of the coupler and through the arms. This type of coupler has already been studied in [27]. As shown in Fig. 4, the rectifier consists of two sub-rectifying circuits and a BLCoupler with a grounded isolation port. In the analysis, the sub-rectifiers are assumed to be identical, and the loss of the BLCoupler is ignored. Based on [27] and [39], the scattering matrix of the BLCoupler is given by the following form:

$$[S] = \frac{-1}{\sqrt{2}} \begin{bmatrix} 0 & j & 1 & 0 \\ j & 0 & 0 & 1 \\ 1 & 0 & 0 & j \\ 0 & 1 & j & 0 \end{bmatrix}. \quad (11)$$

It can be proved that the power loss of the rectifier circuit with the BLCoupler is as follows:

$$P_{lossBL} = \frac{1}{2}|\Gamma|^2 |\Gamma'|^2 |a_1|^2, \quad (12)$$

where Γ and Γ′ are the reflection coefficients at the corresponding power, and a1 is the input wave to the coupler. Therefore, it can be concluded that the efficiency ηPinc at the incident power of Pinc is as follows:

$$\text{for BLCoupler: } \eta_{P_{inc}} = \frac{P_{in} \times \eta_{P_{in}}}{P_{inc}} = (1 - |\Gamma'|^2 |\Gamma|^2) \times \eta_{P_{in}}, \quad (13)$$

since $0 < |\Gamma| < 1$ and $0 < |\Gamma'| < 1$, it is indicated that the RF-DC conversion efficiency can be enhanced by applying the BLCoupler configuration than TCoupler and WDCoupler.

D. CLCoupler and LCoupler

When two transmission lines are adjacent to each other, electromagnetic field interactions can cause power to couple from one line to another. Such lines are referred to as

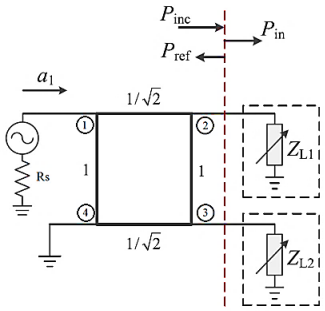

Fig. 4. The rectifier based on the BLCoupler with grounded isolation port.

coupled-line couplers (CLCouplers). The CLCouplers are usually symmetric, meaning that the two conductive strips have the same position and width relative to the ground. This symmetric layout simplifies the analysis of their characteristics. However, the coupling of a CLCoupler is too loose. A Lange coupler (LCoupler) is a practical implementation that achieves high coupling between edge-coupled lines by using multiple parallel lines [39]. The rectifiers based on the CLCoupler and LCoupler with the grounded isolation port are shown in Fig. 5(a) and 5(b). According to [39], the scattering matrix of the quadrature CLCoupler and LCoupler is:

$$[S] = \begin{bmatrix} 0 & j\sqrt{1-c^2} & c & 0 \\ -j\sqrt{1-c^2} & 0 & 0 & c \\ c & 0 & 0 & -j\sqrt{1-c^2} \\ 0 & c & -j\sqrt{1-c^2} & 0 \end{bmatrix}. \quad (14)$$

where c is the voltage coupling coefficient, for example, between ports 3 and 1.

For an analysis of the couplers, at first, the input wave a1 transmits to ports 2 and 3, and then from these ports will be returned to other ports. Similar to the BLCoupler, we can prove the following equations:

$$P_{lossCL} \;\&\; P_{lossL} = \frac{1}{2}[(2c^2|a_1||\Gamma| - 1)^2] + \frac{1}{2}[16c^4(1-c^2)^2|\Gamma|^2|\Gamma'|^2]|a_1|^2 \quad (15)$$

if $0.7 < c < 1$, the second term in the above equation is ten times larger than the first term, so we have approximately efficient:

$$\text{for CLCoupler \& LCoupler: } \eta_{P_{inc}} = \frac{P_{in} \times \eta_{P_{in}}}{P_{inc}} \cong (1 - 16c^4(1-c^2)^2|\Gamma|^2|\Gamma'|^2) \times \eta_{P_{in}}. \quad (16)$$

Since $16C^4(1-C^2)^2 < 1$, the improved efficiency by the CLCoupler and LCoupler in the incident power of Pinc can be obtained than mentiond previous couplers. Of course, it is expected to have a higher efficiency in LCoupler than CLCoupler because of the higher voltage coupling coefficient. On the other hand, the design methods of a coupler are presented in [39] based on the characteristic impedance (Z0), even- (Z0e) and odd- (Z0o) mode impedances of coupled adjacent lines in terms of the strip width and the gap between strips. The voltage coupling coefficient based on this theory can be determined by the following equations:

$$Z_0^2 = Z_{0e}Z_{0o} \;.\; c = \frac{Z_{0e}-Z_{0o}}{Z_{0e}+Z_{0o}}. \quad (17)$$

since, the odd and even mode impedance depends on the physical structure of the coupled lines, the LCoupler may be driving lower impedances than the CLCoupler and so more power transfer as possible.

For $0 < c < 0.7$, the input wave of a1 directly affects the efficiency, and it is not suitable for low input power. Thus, the CLCoupler is most suitable for high voltage coupling factors or high input power.

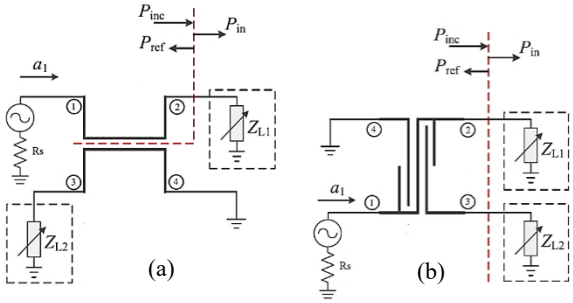

Fig. 5. The rectifier based on a) the CLCoupler and b) LCoupler with grounded isolation port.

III. Rectifier Design and Performance Comparison of Couplers

A. Rectifier Design

To confirm the mentioned theoretical analysis, the designed layout in Fig. 1 has used the various couplers in the rectifier circuit design with the following methodology.

Step 1: According to [20] and [27], a modified single rectifier is designed and developed for maximum efficiency at 2.45 GHz. The level of power is improved between -5 dBm and +5 dBm for medium-power applications, and the designed system can also be used for low and high-power applications, by selecting suitable rectifying diodes. The configuration of the adapted rectifying structure is shown in Fig. 6 (a). It is composed of an MN, rectifying Schottky diodes, and a DC-pass filter. Proper Schottky diodes HSMS2850 are chosen for the rectifying circuit because of the reversed input impedance trend. Note that when the level of input power is more than the finest power of the rectifier, the most power is consumed by the Schottky diodes due to the diode breakdown. The MN converts the complex impedance to 50-Ω, and the DC-pass filter with harmonic rejection is designed using harmonic termination. The DC-pass filter is realized with two fan-shaped branches with different radius, followed by a resistive load (R_L) to excerpt the DC power.

Step 2: According to the analysis in Section II, an appropriate coupler is designed and optimized to operate at

the operating frequency. Actually, the couplers are designed based on quarter-wavelength impedance matching principles. Key design considerations include operating frequency, impedance matching, insertion loss, power division, isolation, and bandwidth. Optimization is achieved using advance design system (ADS) as an electromagnetic simulation software, ensuring high performance in practical applications. It is expected that the rectifier performance is affected by the coupler. The various couplers are applied in the proposed design, with the structures shown from Fig. 6 (b) to Fig. 6 (f) with the optimized physical dimensions. It is worth noting that the optimal dimensions of each coupler are obtained based on a separate design. Their combination with the rectifier is re-optimized to achieve optimal performance. Therefore, the output of their results with the rectifier combination is more important than their individual output.

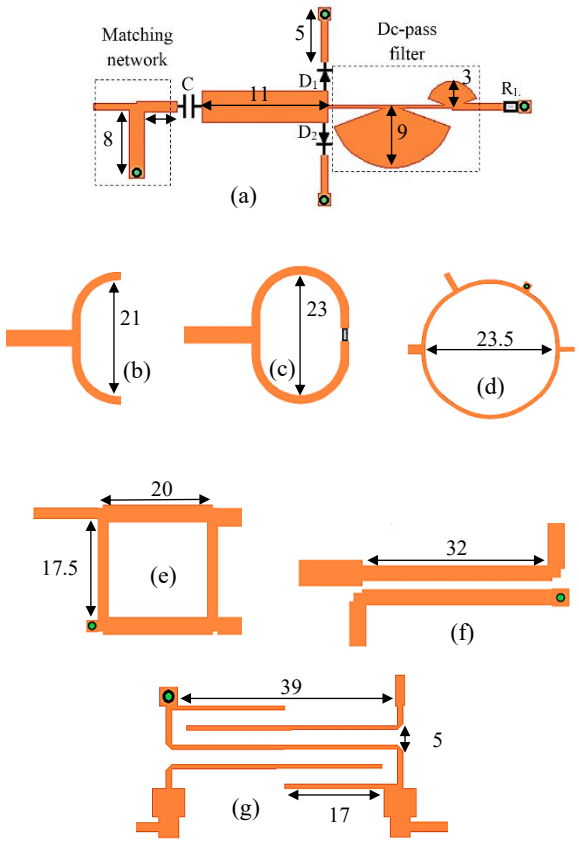

Fig. 6. Geometry of the designs in the proposed circuit with the optimized physical dimensions. (a) Single rectifier; (b) TCoupler; (c) WDCoupler. (d) RRCoupler; (e) BLCoupler; (f) CLCoupler; (g) LCoupler with grounded isolation port. Dimensions are in mm.

Step 3: Two identical single rectifiers are adjoined to the coupler output ports in order to the reflected power can be recycled and the conversion efficiency can be improved in different operating frequencies, input powers, and loads.

In the presented design, the substrate is Rogers-4003, with a thickness of 0.8 mm, a dielectric constant of 3.55, and a loss tangent of 0.0027. It should be illustrated that in the simulation model, the losses of the microstrip line and diodes are considered, and the capacitor models are from MURATA.

B. Simulated Results and Comparison

At first, in order to verify the rectifier circuit performance based on the different couplers, the reflection coefficient |S11| versus operating frequency is shown and compared with Fig. 7. It can be seen that a single rectifier without the coupler (SRWC) is also designed for comparison. It is clear that the rectifier with the various couplers has a smaller reflection coefficient than SRWC. Therefore, the loss of power due to impedance mismatch is decreased by applying the coupler, as indicated in Section II. As shown in Fig. 7, bandwidth for |S11| < -10 dB is increased from 0.05 GHz to 0.23 GHz by applying the proposed technique with the CLCouple, LCoupler, and RRcoupler. Furthermore, the frequency bandwidth can be more extended to 0.3 GHz by using the BLcoupler and Toupler than the other one.

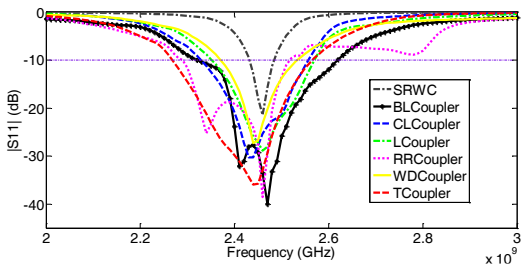

Fig. 7. The |S11| of the rectifiers in terms of operating frequency with the various couplers.

Fig. 8 demonstrates the RF-DC efficiency comparison between the rectifiers based on the different couplers regarding operating frequency, output load, and input power. The losses of the different couplers, such as mismatch loss, isolation loss, dissipative loss, cascade loss, and transmission loss, are taken into the simulation. As illustrated in Fig. 8(a), the conversion efficiency is significantly affected by using the different couplers, so that the efficiency of the rectifier with the BLCoupler is higher than other designs when the input power level is very low or around 0 dBm and more so for maximum efficiency. Nevertheless, from -15 dBm to -5 dBm, the efficiency of the rectifier with the LCoupler is more than other couplers, and then the CLCoupler is better. It should be mentioned that this research on the condition of operating in which the breakdown voltage is not reached, has been focused. Therefore, as shown in Fig. 8(a), the loss of power in the breakdown diodes is highly increased. The TCoupler, RRCouple, and WDCoupler have relatively similar performance in the efficiency of input power, while they have lower efficiency in the performance area compared with previous couplers. The diode breakdown voltage happens later because of lower power loss in these couplers.

The rectifiers using TCoupler, RRCoupler, and WDCoupler work at a higher power level; therefore these rectifiers achieve higher maximum efficiency at the higher power levels, although the focus of this article is on low-level powers. The input power range for over 60% efficiency of the rectifier with TCoupler is from 5.4 dBm to 14.6 dBm, while with the BLCoupler is from 3.8 dBm to 10.2 dBm. The difference in the efficiency of the rectifier with various couplers is primarily because of the rectifier matching in terms of the reflection coefficient and the re-used power. As illustrated in Fig. 8(b), the rectifier with BLCoupler exhibits a higher efficiency (over 60%) in a wide range of load than the other couplers when the output load changes from 210 Ω to 1190 Ω. While, within the output load range of 170 Ω to 490 Ω, the rectifier with the CLCoupler has a higher efficiency in a lower range of output load. As shown in Fig. 8(c), the rectifier based on the BLCoupler has the broadest frequency bandwidth from 2.05 GHz to 2.89 GHz (over 60% efficiency) as compared with the others, while the rectifier based on the CLCoupler has the lowest frequency bandwidth. For better comparison, Table 1 shows the important rectifier parameters based on different coupler structures for efficiency over 60%. Therefore, it can be seen in Table 1 that the rectifier based on the BLCoupler can work in the broader ranges of operating frequency and output load, while it is more sensitive to lower input power level (3.8 dBm) in comparison with the other couplers. Obviously, if input power range was the criterion for superiority, TCoupler is superior to the others with a range of more than 9 dBm.

V. Prototype of Rectifier Based on Blcoupler

For validation, a rectifier circuit with the BLCoupler is designed, optimized, and then fabricated, as shown in Fig. 9. The dimensions of the design are shown in same Fig. 9. The

The fabricated rectifier is characterized and compared with simulation as a function of RF-DC conversion efficiency in terms of output load, operating frequency, and input power. Fig. 10 shows the experimental measurement setup, in which the measurement is extracted by a multi-meter. The measured conversion efficiency can be obtained by:

$$\eta(\%) = \frac{P_{out1}+P_{out2}}{P_{in}}. \quad (18)$$

Pout1 and Pout2 are the output power of the two sub-rectifying networks, and Pin is the input power delivered by a signal generator and a power amplifier. The output powers can be obtained by:

$$P_{out1} = \frac{P_{out1}+P_{out2}}{P_{in}}. \quad (19)$$

$$P_{out1} = \frac{V_{dc1}^2}{R_L}. P_{out2} = \frac{V_{dc2}^2}{R_L}. \quad (20)$$

The 330 pF capacitor (C) and the 360 Ω output load (R_L) are used in the proposed design.

Vdc1 and Vdc2 are the DC output voltage on the loads R_L of the two sub-rectifiers. Note that the two output ports can

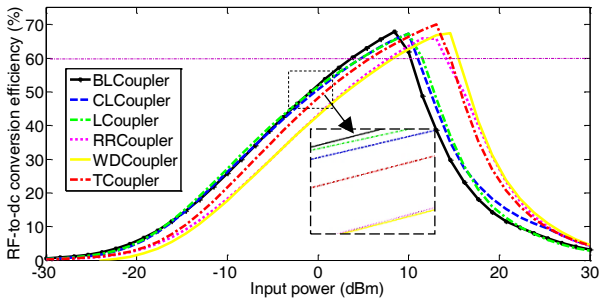

(a)

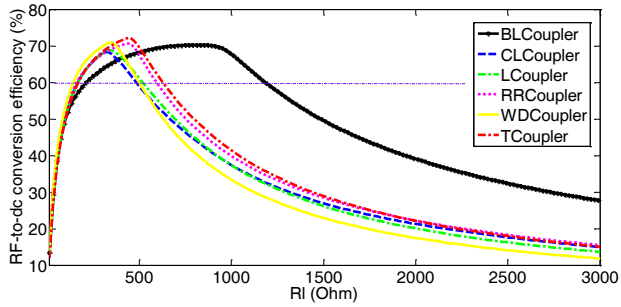

(b)

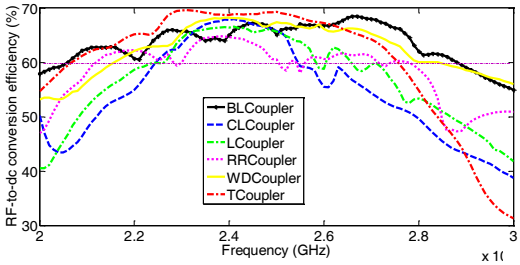

(c)

Fig. 8. The RF-DC efficiency of the rectifiers with the various couplers in terms of (a) input power, (b) output load, and (c) operating frequency.

TABLE. I COMPARISON AMONG RECTIFIER WITH VARIOUS COUPLERS FOR EFFICIENCY OVER 60%.

Type of coupler	Input power (dBm)	Output load (Ω)	Operating frequency (GHz)
BLCoupler	3.8-10.2	210-1190	2.05-2.89
CLCoupler	4.5-10.9	170-490	2.24-2.55
LCoupler	4.5-11.5	170-530	2.24-2.66
RRCoupler	8.2-14.3	150-590	2.12-2.78
WDCoupler	8.3-15.3	130-510	2.15-2.86
TCoupler	5.4-14.6	170-630	2.07-2.76

also be linked together with a DC-DC converter in series or parallel.

The simulated and measured results of conversion efficiencies of the rectifier circuit versus operation frequency, input power level, and output load are shown in Fig. 11. As depicted, the simulated results agree with the measured results, which validate the rectifier circuit design. The minor variance is due to the diode model inaccuracy and the fabrication tolerance. As observed in Fig. 11(a), the

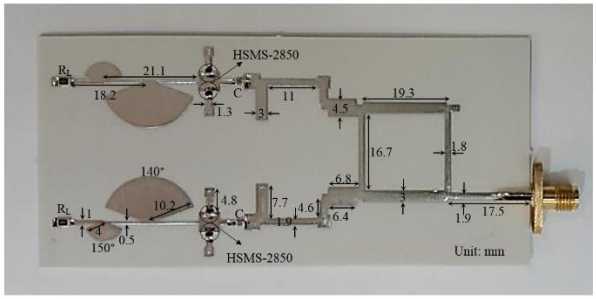

Fig. 9. Layout of the rectifier circuit based on the BLCoupler.

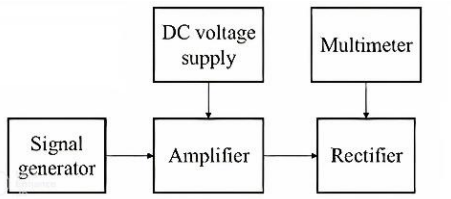

Fig. 10. Schematic of the measurement setup of the rectifier.

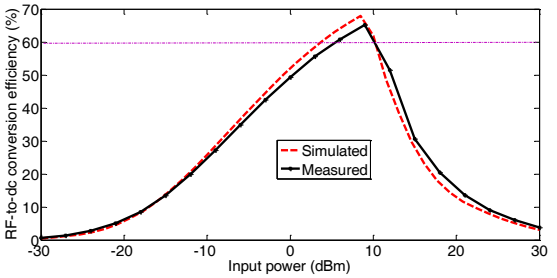

(a)

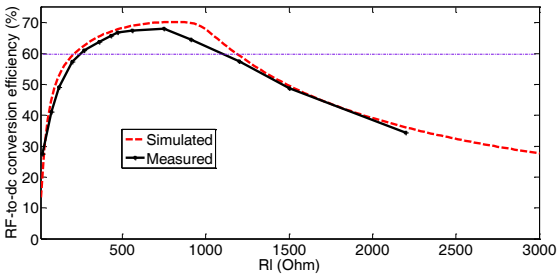

(b)

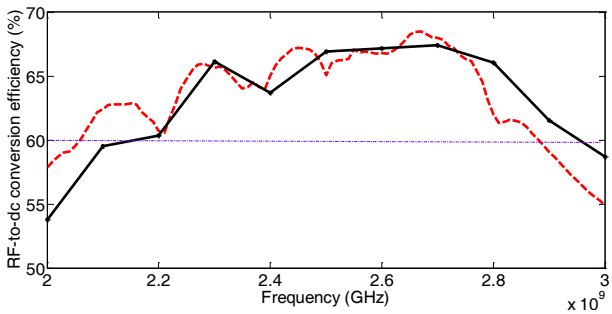

(c)

Fig. 11. Measurement and simulation efficiencies of the rectifier with the BLCoupler in terms of a) input power, b) versus output load for Pin = 9 dBm, and c) operating frequency for Pin = 8 dBm.

rectifier remains above 60% measured RF-DC efficiency from 5.3 to 10.6 dBm, containing a 5.3 dB range of input power for over 60% efficiency with a peak efficiency of 66% at 9 dBm. Moreover, the measurement and simulation efficiencies in term of output load are shown in Fig. 11(b). The rectifier can keep high RF-DC efficiency (over 60%) for a broader range of output load from 200 Ω to 1130 Ω. It can also be observed from Fig. 11(c), that the more than 60% measurement RF-dc efficiency of the rectifier circuit can be obtained in a wideband range from 2.16 GHz to 2.96 GHz (32% fractional bandwidth). These results indicate better performance of the rectifier.

In Table 2, a comparison between the proposed rectifier based on BLCoupler and recent prior works is shown. The proposed circuit has been compared for RF-dc conversion efficiency more than 60%. The proposed work can realize wide input power range, output load range, operating frequency bandwidth with relatively high rectifying efficiency at the same time, while previous works only focus on extending the operating input power range or frequency bandwidth of the rectifiers. Although the efficiency is not the highest one, but it is sensitive at a lower power level, which is an advantage.

TABLE. II PERFORMANCE COMPARISON WITH RELATED RECTIFIERS IN RECENT LITERATURE.

Ref.	[12]	[13]	[36]	This work
Diode model	HSMS282B	HSMS2820 + NE3210S01	HSMS2820 + HSMS2860	HSMS2850
Substrate	RO4003C	RT_Duroid5880	(ε_r=2.65) N.S*	Rogers-4003
Operating frequency for efficiency over 60% (GHz)	4.8-6.2	2.45	2.45	2.16-2.96
Output load for efficiency over 60% (Ω)	160-800	80-520	N.S	200-1130
Input power for efficiency over 60% (dBm)	15-27.5	18.5-33	12-25	5.3-10.6
Maximum efficiency @ Input power	74.1% @ 23dBm	74.4% @ 30dBm	75.5% @ 13dBm	66% @ 9dBm

*Not Stated

IV. Implementing the Rectifier Circuit in MPT Systems

The practical implementation of a rectifier circuit in MPT systems necessitates addressing multiple engineering and operational challenges to optimize performance and reliability. By incorporating advanced design techniques and adhering to established standards, rectifier circuits can facilitate the reliable deployment of MPT systems for

various applications. Some of the important implementation challenges are as follows:

Efficiency Optimization: the rectification process should maximize the conversion efficiency to ensure minimal energy loss. Diode selection, matching networks, and load optimization are key factors influence efficiency [40].

Power Handling and Thermal Management: MPT systems often operate at high power levels, making thermal management a crucial design consideration. The rectifier circuit should incorporate heat sinks or advanced cooling techniques to prevent thermal degradation [41]. Moreovere, the nonlinear characteristics of diodes may cause efficiency degradation at high power levels, necessitating careful circuit design [42].

Harmonic Suppression and Electromagnetic Interference (EMI) Mitigation: Harmonics generated during rectification can interfere with nearby communication systems and reduce rectifier efficiency. Filtering, shielding, and grounding techniques can significantly suppress unwanted frequencies and improve system stability [43].

Environmental Robustness: The rectifier circuit should be designed to withstand external environmental factors, such as resistance in temperature and humidity, and mechanical reliability [44].

Antenna Integration and Beam Alignment: The rectifier's integration with the receiving antenna affects overall system performance. Misalignment can reduce power reception efficiency, requiring adaptive control mechanisms [42].

V. Conclusion

This article has presented and introduced a study on various couplers in the rectifier circuit topology to design optimized high-efficiency rectifier circuits with an extended range of frequency bandwidth, output load, and input power. The design principles of different couplers have been analyzed, and closed-form design formulas have been derived. Furthermore, the mechanism and design procedure of the rectifier with and without coupler have been presented and compared. Among the various couplers, the rectifier based on the BL Coupler demonstrates superior RF-DC conversion efficiency across a wider frequency band and output load range. Therefore, to validate the approach, the designed rectifier operating at 2.33–2.63 GHz, based on the BL Coupler, was implemented and fabricated. The rectifier achieves over 60% efficiency within the 2.16–2.96 GHz range, with an input power range of 5.3 dBm to 10.6 dBm. The measurement results confirm the effectiveness of the proposed method for designing rectifiers. Additionally, this approach can be applied to other scenarios.

REFERENCES

[1] F. Geran, N. Mirzababaee, and S. Mohanna, "RF power harvester using a broadband monopole antenna and a quad-band rectifier," *International Journal of Industrial Electronics Control and Optimization*, vol. 4, no. 1, pp. 59-65, 2021.

[2] H. Xiong, Q. Yang, Y.-Z. Huang, X. Wang, Z. Yi, and H.-Q. Zhang, "A high-efficiency hybrid microwave power receiving metasurface array with dual matching of surface impedance and phase gradient," *Applied Physics Letters*, vol. 125, no. 4, 2024.

[3] M. M. Fakharian, "A dual circular and linear polarized rectenna for RF energy harvesting at 0.9 and 1.8 GHz GSM bands," *Electromagnetics*, vol. 41, no. 8, pp. 545-556, 2021.

[4] M. M. Fakharian, "A wideband rectenna using high gain fractal planar monopole antenna array for RF energy scavenging," *International Journal of Antennas and Propagation*, vol. 2020, pp. 1-10, 2020.

[5] M. M. Fakharian, "A wideband fractal planar monopole antenna with a thin slot on radiating stub for radio frequency energy harvesting applications," *International Journal of Engineering*, vol. 33, no. 11, pp. 2181-2187, 2020.

[6] J. Alirio and B. C. Nuno, "A batteryless RFID remote control system," *IEEE Transactions on Microwave Theory and Techniques*, vol. 61, no. 7, pp. 2727-2736, 2013.

[7] J. Guo, H. Zhang, and X. Zhu, "Theoretical analysis of RF-DC conversion efficiency for class-F rectifiers," *IEEE Transactions on Microwave Theory and Techniques*, vol. 62, no. 4, pp. 977-985, 2014.

[8] S. Ladan and K. Wu, "Nonlinear modeling and harmonic recycling of millimeter-wave rectifier circuit," *IEEE Transactions on Microwave Theory and Techniques*, vol. 63, no. 3, pp. 937-944, 2015.

[9] M. Roberg, T. Reveyrand, I. Ramos, E.A. Falkenstein, and Z. Popović, "High-efficiency harmonically terminated diode and transistor rectifiers," *IEE IEEE Transactions on Microwave Theory and Techniques*, vol. 60, no. 12, pp. 4043-4052, 2012.

[10] C. Wang, N. Shinohara, and T. Mitani, "Study on 5.8-GHz single-stage charge pump rectifier for internal wireless system of satellite," *IEEE Transactions on Microwave Theory and Techniques*, vol. 65, no. 4, pp. 1058-1065, 2017.

[11] Q. Zhang, J-H. Ou, Z. Wu, and H-Z. Tan, "Novel microwave rectifier optimizing method and its application in rectenna designs," *IEEE Access*, vol. 6, pp. 53557-53565, 2018.

[12] H. Zeng, Y. Tang, and Y. Liu, "Compact high-efficiency c-band rectifier with high input power for microwave power transmission," *Electronics Letters*, vol. 59. e12776, 2023.

[13] H. Xiao, H. Zhang, W. Song, J. Wang, W. Chen, and M. Lu, "A High-Input Power Rectifier Circuit for 2.45-GHz Microwave Wireless Power Transmission," *IEEE Transactions on Industrial Electronics*, vol. 69, no. 3, pp. 2896-2903, March 2022.

[14] J. Kimionis, A. Collado, M.M. Tentzeris, and A. Georgiadis, "Octave and decade printed UWB rectifiers based on nonuniform transmission lines for energy harvesting," *IEEE Transactions on Microwave Theory and Techniques*, vol. 65, no. 11, pp. 4326-4334, 2017.

[15] M. Mansour, X.L. Polozec, and H. Kanaya, "Enhanced broadband RF differential rectifier integrated with archimedean spiral antenna for wireless energy harvesting applications," *Sensors*, vol. 19, no. 3, pp. 1-13, 2019.

[16] M. Nariman, F. Shirinfar, S. Pamarti, A. Rofougaran, and F.D. Flaviis, "High-efficiency millimeter-wave energy-harvesting systems with milliwatt-level output power,"

IEEE Transactions on Circuits and Systems II, vol. 64, no. 6, pp. 605-609, 2017.
[17] Y. L. Lin, X. Y. Zhang, Z.-X. Du, and Q. W. Lin, "High-efficiency microwave rectifier with extended operating bandwidth," *IEEE Transactions on Circuits and Systems II*, vol. 65, no. 7, pp. 819-823, 2017.
[18] J. Liu, X. Y. Zhang, and C. L. Yang, "Analysis and design of dual-band rectifier using novel matching network," *IEEE Transactions on Circuits and Systems II,* vol. 65, no. 2, pp. 431-435, 2018.
[19] M. M. Fakharian, "A compact UWB antenna with dynamically switchable band-notched characteristic using broadband rectenna and DC-DC booster," *International Journal of Microwave and Wireless Technologies*, vol. 13, no. 10, pp. 1086-1095, 2021.
[20] Y. Huang, N. Shinohara, and T. Mitani, "A constant efficiency of rectifying circuit in an extremely wide load range," *IEEE Transactions on Microwave Theory and Techniques* vol. 62, no. 4, pp. 986-993, 2014.
[21] Y. Lu, H. J. Dai, M. Huang, M.-K. Law, S.-W. Sin, S.-P. U, and R.P. Martins, "A wide input range dual-path CMOS rectifier for RF energy harvesting," *IEEE Transactions on Circuits and Systems II*, vol. 64, no. 2, pp. 166-170, 2017.
[22] T. W. Barton, J. Gordonson, and D. J. Perreault, "Transmission line resistance compression networks and applications to wireless power transfer," *IEEE Journal of Emerging and Selected Topics in Power Electronics, v*ol. 3, no. 1, pp. 252-260, 2015.
[23] S. H. Abdelhalem, P.S. Gudem, and L.E. Larson, "An RF-dc converter with wide-dynamic-range input matching for power recovery applications," *IEEE Transactions on Circuits and Systems II, Express. Briefs*, vol. 60, no. 6, pp. 336-340. 2013.
[24] X. Y. Zhang and Q.-W. Lin, "High-efficiency rectifier with extended input power range based on two parallel sub-rectifying circuits," *IEEE International Wireless Symposium*, Shenzhen, China, Match 2015, pp. 1-4.
[25] Z.-X. Du and X. Y. Zhang, "High-efficiency microwave rectifier with less sensitivity to input power variation," *IEEE Microwave and Wireless Components Letters*, vol. 27, no. 11, pp. 1001-1003, 2017.
[26] Y. Y. Xiao, Z.-X. Du, and X. Y. Zhang, "High-efficiency rectifier with wide input power range based on power recycling," *IEEE Transactions on Circuits and Systems II: Express. Briefs,* vol. 65, no. 6, pp. 744-748, 2018.
[27] X. Y. Zhang, Z.-X. Du, and Q. Xue, "High-efficiency broadband rectifier with wide ranges of input power and output load based on branch-line coupler," *IEEE Transactions on Circuits and Systems I: Reg. Papers*, vol. 64, no. 3, pp. 731-739, 2016.
[28] M. Huang, Y. L. Lin, J.-H. Ou, X. Y. Zhang, Q. W. Lin, W. Che, and Q. Xue, "Single- and dual-band RF rectifiers with extended input power range using automatic impedance transforming," *IEEE Transactions on Microwave Theory and Techniques*, vol. 67, no. 5, pp. 1974-1984, 2019.
[29] K. Niotaki, A. Georgiadis, A. Collado, and J. S. Vardakas, "Dual-band resistance compression networks for improved rectifier performance," *IEEE Transactions on Microwave Theory and Techniques*, vol. 62, no. 12, pp. 3512-3521, 2014.
[30] M. M. Fakharian, "A high gain wideband circularly polarized rectenna with wide ranges of input power and output load," *International Journal of Electronics,* vol. 109, no. 1, pp. 83-99, 2021.
[31] V. Marian, C. Vollaire, J. Verdier, and B. Allard, "Potentials of an adaptive rectenna circuit," *IEEE Antennas and Wireless Propagation Letters*, vol. 10, pp. 1393-1396, 2011.
[32] C. J. Li and T. C. Lee, "2.4-GHz high-efficiency adaptive power harvester," *IEEE Transactions on Very Large Scale Integration Systems,* vol. 22, no. 2, pp. 434-438, 2014.
[33] Z. Liu, Z. Zhong, and Y.-X. Guo, "Enhanced dual-band ambient RF energy harvesting with ultra-wide power range," *IEEE Microwave and Wireless Components Letters*, vol. 25, no. 9, pp. 630-632, 2015.
[34] Z. Du, S. F. Bo, Y. F. Cao, J. Ou, and X. Y. Zhang, "Broadband circularly polarized rectenna with wide dynamic-power-range for efficient wireless power transfer," *IEEE Access*, vol. 8, pp. 80561-80571, 2020.
[35] M. M. Fakharian, "RF energy harvesting using high impedance asymmetric antenna array without impedance matching network," *Radio Science*, vol. 56, no. 3, pp. 1-10, 2021.
[36] C. Peng, Z. Ye, J. Wu, C. Chen, and Z. Wang, "Design of a wide-dynamic RF-DC Rectifier circuit based on an unequal wilkinson power divider," *Electronics*, vol. 10, p. 2815, 2021
[37] V. Marian, B. Allard, C. Vollaire, and J. Verdier, "Strategy for microwave energy harvesting from ambient field or a feeding source," *IEEE Transactions on Power Electronics, vol. 27, n*o. 11, pp. 4481-4491, 2012.
[38] Non RF applications for surface mount schottky diode pairs HSMS2850, Datasheet, Avago Technol., San Jose, CA, USA, May 2010.
[39] D. M. Pozar, Microwave engineering, 4th edition. New York, NY, USA: Wiley, 2012.
[40] J. Huang, Y. Zhou, Z. Ning, and H. Gharavi, "Wireless Power transfer and energy harvesting: current status and future prospects," *IEEE Wireless Communications*; vol. 26, no. 4, pp. 1-7, 2019.
[41] X. Zhu, K. Jin, Q. Hui, W. Gong, and D. Mao, "Long-range wireless microwave power transmission: a review of recent progress," *IEEE Journal of Emerging and Selected Topics in Power Electronics*, vol. 9, no. 4, pp. 4932-4946, 2021.
[42] N. Shinohara, Wireless power transfer via radiowaves. John Wiley & Sons, 2014.
[43] D. Kobuchi, G. E. Moore, Y. Narusue and J. R. Smith, "Suppression of receiver harmonic currents in wireless power transfer systems," *IEEE Wireless Power Technology Conference and Expo*, San Diego, USA, 2023, pp. 1-5.
[44] P. Lazzeroni, V. Cirimele, and A. Canova, "Economic and environmental sustainability of Dynamic Wireless Power Transfer for electric vehicles supporting reduction of local air pollutant emissions," *Renewable and Sustainable Energy Reviews*, vol. 138, pp. 1-15, March 2021.

Mohammad M. Fakharian was born in Tehran, Iran, in 1987. He received the B.S., M.S., and Ph.D. degrees in Electrical Engineering from Semnan University, Semnan, Iran, in 2009, 2012, and 2016, respectively. Currently, he is an associate professor at the University of Garmsar, Garmsar, Iran. His research interests include low-profile printed and patch antennas for wireless communication, fractal, miniature, and multiband antennas, meta-materials and EBG structures interaction with antennas and RF passive components, reconfigurable antennas, RF energy harvesting, and electromagnetic theory: numerical methods and optimization techniques.